

MOL # 89409

## **Mechanism of action of novel lung oedema therapeutic AP301 by activation of ENaC**

Shabbir W, Scherbaum-Hazemi P, Tzotzos S, Fischer B, Fischer H, Pietschmann H, Lucas  
R, Lemmens-Gruber R

*Department of Pharmacology and Toxicology, University of Vienna, Althanstrasse 14, A-  
1090 Vienna, Austria (S.W., S.-H.P., L.-G.R.)*

*APEPTICO Forschung und Entwicklung GmbH, Mariahilferstrasse 136, A-1150 Vienna,  
Austria (T.S., F.B., F.H., P.H.)*

*Vascular Biology Center, Dept. of Pharmacology and Toxicology, Division of Pulmonary  
Medicine, Medical College of Georgia, Georgia Regents University, 1459 Laney-Walker  
Boulevard, Augusta, GA 30912-2500, USA (L.R.)*

MOL # 89409

**Running title:** AP301-induced activation of hENaC

To whom correspondence should be addressed. Phone: +43 1 4277 55309. FAX:

+43 1 4277 9553. Email: [waheed.shabbir@univie.ac.at](mailto:waheed.shabbir@univie.ac.at)

## COUNTS

Text pages: 25

Tables: 1

Figures: 7

References: 59

Abstract: 252 words

Introduction: 712 words

Discussion: 1608 words

**ABBREVIATIONS:** AFC, alveolar fluid clearance; ALF, apical alveolar lining fluid; ALI, acute lung injury; ARDS, acute respiratory distress syndrome; AT1 and ATII cells, alveolar type I and type II cells; CFTR, cystic fibrosis transmembrane conductance regulator; CNG, cyclic-nucleotide-gated cation; ENaC, epithelial sodium channel; hNE, neutrophil elastase; PNGase F, Peptide-*N*<sup>4</sup>-(*N*-acetyl- $\beta$ -D-glucosaminyl)asparagine amidase F; *P*<sub>o</sub>, open probability; TEA, tetraethylammonium chloride; TIP, lectin-like domain of tumour necrosis factor

MOL # 89409

## ABSTRACT

AP301, a cyclic peptide, comprising the human tumour necrosis factor lectin like domain (TIP domain) sequence, is currently being developed as a therapy for lung oedema and has been shown to reduce extravascular lung water and improve lung function in a mouse, rat and pig model. The current paradigm for liquid homeostasis in the adult mammalian lung is that passive apical uptake of sodium via the amiloride-sensitive epithelial sodium channel (ENaC) and non-selective cyclic-nucleotide-gated cation (CNG) channels, creates the major driving force for reabsorption of water through the alveolar epithelium besides other ion channels such as potassium and chloride channels. AP301 can increase amiloride-sensitive current in A549 cells as well as in freshly isolated type II alveolar epithelial cells from different species; in all these cell types ENaC is expressed endogenously. Consequently, the present study was undertaken to determine whether ENaC is the specific target of AP301. The effect of AP301 in A549 cells and in HEK and CHO cells heterologously expressing human ENaC subunits ( $\alpha$ ,  $\beta$ ,  $\gamma$  and  $\delta$ ) was measured in patch clamp experiments. Also the congener TIP peptide AP318 activated ENaC by increasing single channel open probability. AP301 increased current in proteolytically activated (cleaved) but not near silent (uncleaved) ENaC in a reversible manner. For maximal activity  $\alpha\beta\gamma$ - or  $\delta\beta\gamma$ -ENaC co-expression was required. After deglycosylation of extracellular domains of ENaC, no increase in current was observed. Thus, our data suggest that specific interaction of AP301 with both endogenously and heterologously expressed ENaC requires precedent binding to glycosylated extracellular loop(s).

## INTRODUCTION

Regulation of  $\text{Na}^+$  and  $\text{Cl}^-$  transport across the alveolar epithelium is crucial to lung fluid homeostasis. Ion channels and other transport proteins in the membranes of alveolar type I (ATI) and type II (ATII) cells are involved in controlling the flow of ions between the apical alveolar lining fluid (ALF) and the basolateral interstitium. Cation channels include the amiloride-sensitive epithelial  $\text{Na}^+$  channel (ENaC), which plays a key role in lung liquid balance (Folkesson and Matthay, 2006; Berthiaume and Matthay, 2007; Eaton et al., 2009). Nonselective cyclic-nucleotide-gated (CNG) cation channels also conduct  $\text{Na}^+$  ions and thereby contribute to lung liquid clearance (Wilkinson et al., 2011). The main function of  $\text{K}^+$  channels, characterised by their high selectivity for  $\text{K}^+$  over  $\text{Na}^+$  (>100 to 1) is to control membrane potential thereby maintaining the electrochemical gradient necessary for ion and fluid transport (Bardou et al., 2009). Chloride channels, including the cystic fibrosis transmembrane conductance regulator (CFTR), which plays a central role in alveolar ion transport (Lazrak et al., 2011), and other less well-characterised  $\text{Cl}^-$  channels, such as the ionotropic  $\gamma$ -aminobutyric acid type A ( $\text{GABA}_A$ ) receptor (Jin et al., 2006), voltage-gated  $\text{Cl}^-$  channels, CLC5 and CLC2 and a basolaterally located  $\text{Cl}^-$  channel (Berger et al., 2010), also contribute to lung liquid homeostasis (Hollenhorst et al., 2011).

The current paradigm for liquid homeostasis in the adult mammalian lung is that passive apical uptake of  $\text{Na}^+$  via ENaC and amiloride-insensitive CNG channels, creates the major driving force for reabsorption of water through the alveolar epithelium (Matthay et al., 2005; Folkesson and Matthay, 2006; Berthiaume and Matthay, 2007; Hollenhorst et al., 2011; Wilkinson et al., 2011). An electrochemical gradient is maintained by  $\text{Na}^+/\text{K}^+$ -ATPase, located basolaterally in alveolar epithelial cells, causing  $\text{Na}^+$  to enter the cells through apically located ENaC and CNG channels. Water then follows the osmotic gradient thus created, resulting in its removal from the alveoli and subsequent extrusion into the interstitial space (Johnson et al., 2006). Disruption of these processes occurs in pathologies where permeability of the alveolar epithelium and pulmonary capillary endothelium is increased, leading to excessive accumulation of ALF and oedema (Mutlu and Sznajder, 2005). In acute

MOL # 89409

lung injury (ALI) and acute respiratory distress syndrome (ARDS), improved alveolar fluid clearing capacity has been associated with a better prognosis (Ware and Matthay, 2001).

ENaC is composed of four homologous subunits,  $\alpha$ ,  $\beta$ ,  $\gamma$  and  $\delta$ , each comprising a large extracellular loop lying between two transmembrane domains flanked by short cytoplasmic amino and carboxyl termini (Canessa et al., 1994a; McDonald et al., 1994; Snyder et al., 1994; Althaus et al., 2011). Post-translational modification of ENaC involves proteolytic cleavage of the  $\alpha$ - and  $\gamma$ -subunits (Hughey et al., 2003; Kleyman et al., 2009; Gaillard, 2010) and *N*-glycosylation of the  $\alpha$ ,  $\beta$  and  $\gamma$ -subunits (Snyder et al., 1994; Adams et al., 1997; Hughey et al., 2004a). Cleavage sites for furin and other serine proteases as well as *N*-glycosylation sites occur in the extracellular loops of ENaC subunits. Both extracellular and intracellular proteolysis are believed to participate in ENaC regulation as evidenced by the presence of numerous sites with different susceptibilities to cleavage by trypsin in all three subunits, including sites in the C termini of both  $\beta$ - and  $\gamma$ -subunits (Jovov et al., 2002; Hughey et al., 2004b). Both mature and immature ENaC subunits have been observed at the cell surfaces in stably transfected kidney cells (Hughey et al., 2004a), and 'near-silent' channels in the membranes of cultured fibroblasts expressing ENaC subunits have been identified by their activation following exposure to trypsin (Caldwell et al., 2004). Proteolytic cleavage of ENaC is thought to increase open probability ( $P_o$ ) (Chraibi et al., 1998; Diakov et al., 2008; Gaillard et al., 2010).

The lectin-like domain of tumour necrosis factor, TNF (TIP) and the TIP peptide, a cyclic peptide mimicking this domain (Lucas et al, 1994) effect ALF reabsorption due to their capacity to enhance amiloride-sensitive  $\text{Na}^+$  current in alveolar epithelial cells (Fukuda et al. 2001; Elia et al., 2003; Braun et al., 2005; Vadasz et al., 2008; Hamacher et al., 2010; Hazemi et al., 2010). The oedema-reducing effect of the lectin-like domain involves binding to specific oligosaccharides such as *N,N*-diacetylchitobiose and branched trimannoses (Hribar et al., 1999, Braun et al., 2005).

AP301, a cyclic peptide comprising the human TIP sequence and currently being developed as a therapy for lung oedema (Phase II clinical trials), has been shown to reduce

MOL # 89409

extravascular lung water and improve lung function in a pig model of ALI (Hartmann et al., 2013) and to enhance the amiloride-sensitive  $\text{Na}^+$  current in freshly-isolated ATII cells from dog, pig and rat lungs (Hamacher et al., 2010; Tzotzos et al., 2013). The current-enhancing effect of AP301 is not inhibited by CNG channel blockers, suggesting that AP301 activates  $\text{Na}^+$  current flowing through ENaC (Tzotzos et al., 2013).

ENaC modulators described so far are small molecule compounds such as amiloride (Benos, 1982), phenamil and benzamil (Hirsh et al., 2006), which block channel function, and glibenclamide (Chraïbi and Horisberger, 1999; Schnizler et al., 2003), S3969 (Lu et al., 2008) and LipoxinA<sub>4</sub> (Wang et al., 2013) which activate ENaC. To date, no synthetic peptide of natural origin targeting ENaC has been reported. The present study was undertaken to determine whether ENaC is the target of AP301. Thus, the effect of AP301 on the amiloride-sensitive  $\text{Na}^+$  current in HEK and CHO cells heterologously expressing ENaC subunits ( $\alpha$ ,  $\beta$ ,  $\gamma$  and  $\delta$ ) was measured in patch clamp experiments. These results demonstrate that the TIP peptide AP301 can activate ENaC in heterologous expression systems.

MOL # 89409

## **MATERIALS AND METHODS**

### **cDNA Constructs and Cell Culture**

EGFP tagged cDNAs encoding  $\alpha$ ,  $\beta$ , and  $\gamma$  human (h) ENaC were a kind gift from Dr. Deborah L. Baines, St George's, University of London, London, UK. cDNAs encoding  $\alpha$ ,  $\beta$ , and  $\gamma$  human (h) ENaC were a kind gift from Dr. Peter M Snyder, University of Iowa Carver College of Medicine, Iowa City, USA.  $\delta$ (h) ENaC was a kind gift from Dr. Mike Althaus, Justus-Liebig University, Giessen, Germany.

### **Cell Culture and Transfection**

HEK-293, CHO and RPMI-2650 cells were bought from American Type Cell Culture (ATCC). A549 cells were kindly supplied by W. Berger from the Department of Medicine I, Institute of Cancer Research, Medical University of Vienna, Austria in the 80<sup>th</sup> passage. HEK-293, CHO and A549 cells were cultured in Dulbecco's Modified Eagle's Medium (Invitrogen, Austria) and RPMI 2650 cells were cultured in Eagle's Minimum Essential Medium (ATCC) supplemented with 10% fetal bovine serum (Invitrogen), 100 units/ml penicillin and 100  $\mu$ g/ml streptomycin (Sigma-Aldrich GmbH, Austria).

HEK-293 and CHO cells were transfected with plasmids coding for wild type (WT)  $\alpha$ -,  $\beta$ -,  $\gamma$ - and  $\delta$ -hENaC or indicated subunits combinations, twenty-four hours after seeding using X-treme Gene HP DNA Transfection Reagent (Roche Diagnostics, Mannheim, Germany) according to the manufacturer's protocol. The transfection reagent was used in a ratio 1:3. To avoid excessive sodium loading of the cells, twenty-four hours after transfection, medium was supplemented with (10 $\mu$ M) amiloride (Sigma-Aldrich GmbH, Austria).

### **Electrophysiology**

#### *Whole-cell Patch Clamp*

Whole cell currents were acquired from transfected HEK-293, CHO cells or A549 cells at room temperature (19-22°C) 48-72 h after plating or post transfection using an Axopatch 200B amplifier and Digidata 1440A with pCLAMP10.2 software (Axon Instruments, CA,

MOL # 89409

USA). Currents were recorded at 10 kHz and filtered at 5 kHz. Green fluorescent protein (GFP) was used to facilitate selection of successfully transfected cells. Glass cover slips with the cultured cells were transferred to a chamber of 1 ml capacity, mounted on the stage of an inverted microscope (Zeiss, Axiovert 100). The chamber contained 1 ml of the bath solution of the following composition (in mM): 145 NaCl, 2.7 KCl, 1.8 CaCl<sub>2</sub>, 2 MgCl<sub>2</sub>, 5.5 glucose and 10 HEPES, adjusted to pH 7.4 with 1 M NaOH solution. The borosilicate glass patch pipettes (Harvard Apparatus, Holliston, MA, USA) with resistances of 2–4 MΩ were pulled and polished using a DMZ Universal Puller (Zeitz Instruments, Martinsried, Germany). The pipette solution contained (in mM): 135 potassium methane sulphonate, 10 KCl, 6 NaCl, 1 Mg<sub>2</sub>ATP, 2 Na<sub>3</sub>ATP, 10 HEPES and 0.5 EGTA, adjusted to pH 7.2 with 1 M KOH solution. In ion substitution experiments, NaCl was replaced with equimolar concentrations of N-methyl-D-glucamine (NMDG) chloride. Capacity transients were cancelled, and series resistance was compensated. In whole-cell experiments capacitance was ~9 pF and was routinely compensated. Access resistance were monitored and 75% compensated. Data acquisition and storage were processed directly to a PC.

After GΩ-seal formation, the equilibration period of 5 min was followed by recordings at holding potentials ( $E_h$ ) at –100 mV unless otherwise stated. Gigaseals were continuously monitored during the experiments to avoid inadequate voltage clamp. Aliquots of AP301 stock solution, which was prepared with distilled water, were cumulatively added into the bathing solution, resulting in desired concentrations. Amiloride was added in control experiments in order to identify the amiloride-sensitive Na<sup>+</sup> current from the total current. The wash-in phase lasted about 1 min. After steady-state effects with each indicated compound had been reached, the same clamp protocol was applied as during control recordings. At the end of the experiments with AP301, amiloride was added in order to show whether the peptide-induced increase in current was due to the amiloride-sensitive Na<sup>+</sup> current; in this way the specificity of AP301 compound for the amiloride-sensitive Na<sup>+</sup> current could be proven. In wash-out phase the control solution was applied onto the patched cells after reaching the steady state wash-in phase. The amiloride-sensitive current was determined by



MOL # 89409

subtracting the whole-cell current measured in the presence of amiloride from that measured in the absence of amiloride at given concentration.

### *Single Channel Patch Clamp*

Single channel currents were acquired at room temperature (19-22°C) 48-72 h after plating or post transfection using the outside-out, inside-out and cell attached patch clamp configurations. Five minutes after gigaseal formation control recordings were done in every patch with the same pulse protocol as with the test compound. Single channel currents were recorded using an Axopatch 200B amplifier and Digidata1440A with pCLAMP10.2 software (Axon Instruments, CA, USA). Currents were acquired at 4 kHz and low pass filtered at 1 kHz. The borosilicate glass patch pipettes (Harvard Apparatus, Holliston, MA, USA) with resistances of 10–14 M $\Omega$  were pulled and polished using a DMZ Universal Puller (Zeitz Instruments, Martinsried, Germany). Bath and pipette solutions contained (in mM): 145 potassium methane sulfonate, 5 MgCl<sub>2</sub>, 40 mannitol, 10 HEPES, 5.5 glucose, pH 7.4. Single channel currents were subsequently filtered at 200 Hz and analyzed with pCLAMP10.2. Eventual slow drifts of the baseline were corrected by fitting a non-sloping baseline through each sweep. Single-channel currents and open probability were obtained from the distance of the peak and the areas under the peak of amplitude histograms, respectively. Records were idealized by setting the detection threshold to half of the unitary current amplitude. Open and closed time distributions were fitted using a non-linear least-squares method.

### *Proteolytic cleavage of ENaC*

Experiments were performed with HNEC (RPMI-2650) cells, which express ENaC (Prulière-Escabasse et al., 2010). A lysine residue in the  $\gamma$ -subunit of ENaC ( $\gamma$ K181) has been identified for the activation of near-silent channels in the plasma membrane by extracellular trypsin, chymotrypsin or hNE (Diakov et al. 2008).

RPMI-2650 cells showed very little inward current at -100 mV test pulses. Trypsin (Sigma-Aldrich, Austria) at a concentration of 100  $\mu$ g/ml was applied for 1 to 5 min at room

MOL # 89409

temperature. Thereafter, an increase of inward current was observed. After a steady-state level has been reached trypsin was washed out and control recordings were done for 3 minutes before AP301 was applied at a concentration of 120 nM. Amiloride (10  $\mu$ M) was added at the end of each experiment.

### *Deglycosylation with PNGase F*

Docking and molecular dynamics simulation experiments have indicated that the TIP peptide AP301 represents a partial binding motif for chitobiose (Dulebo et al., 2012). To investigate a possible interaction of the TIP-peptides with sugar moieties on the cell membrane, deglycosylation of the A549 as well as transfected and non-transfected HEK-293 cell membranes was performed with PNGase F at room temperature. Peptide-*N*<sup>4</sup>-(*N*-acetyl- $\beta$ -D-glucosaminyl)asparagine amidase F (PNGase F, peptide *N*-glycanase) is a 34.8-kDa amidohydrolase secreted by *Flavobacterium meningosepticum*. It has been previously shown that 1-5 min treatment of ENaC with PNGase causes the removal of almost all *N*-linked oligosaccharides. PNGase F digestion deaminates the asparagine residue to aspartic acid, and leaves the oligosaccharide intact, keeping it suitable for further analysis. Furthermore, it has been shown previously that all six glycosylation sites in ENaC  $\alpha$ -subunit can be removed with no obvious effect on channel function (Snyder et al., 1994). Currents were recorded in the whole-cell and cell-attached mode, the latter for a more detailed study of the kinetics of channel opening in single channel experiments.

In whole cell mode experiments, A549 and HEK cells were incubated with the enzyme (100 units) for 1-5 minutes immediately prior to the patch clamp measurements and glass cover slips with the cultured cells were rinsed with external solution before being transferred to the chamber of the 1 ml bath. After control recordings, 30 nM TNF- $\alpha$  or 120 and 240 nM AP301 were added to the bath solution in A549 cells and 120 nM AP301 in HEK cells.

In single channel experiments, PNGase F (100 units) was added to the pipette solution. TNF- $\alpha$ , AP301 or AP318 were added to the pipette solution in concentrations corresponding to their respective EC<sub>50</sub> values (8 nM and 60 nM) (Hazemi et al, 2010). For single channel

MOL # 89409

current measurements 10 mM tetraethylammonium chloride (TEA) was additionally added to the pipette solution to block the potassium channel, which has a large amplitude compared to the sodium channel. In this way sodium channel opening could be observed without interference from the potassium channel.

### **Test compounds and chemicals:**

TIP peptides AP301 (Cyclo(CGQRETPEGAEAKPWYC)) and AP318 (Cyclo(4-aminobutanoic acid-GQRETPEGAEAKPWYD)) were obtained from APEPTICO Forschung und Entwicklung GmbH. See Hazemi et al. (2010) for structural details. The test compounds were studied at a concentration range of 3.5 to 240 nM. The stock solutions were prepared with distilled water and stored in the freezer. TNF- $\alpha$  was purchased from Sigma-Aldrich, Saint Louis, USA. Mouse TNF- $\alpha$ , recombinant, expressed in *E. coli* (T 7539) was used. The stock solution with distilled water was prepared and stored in the freezer at -20°C. The reference compound TNF- $\alpha$  was studied at concentrations ranging from 1.75 to 30 nM. TEA was used at a concentration of 10 mM to block the K<sup>+</sup> current. Both amiloride hydrochloride hydrate and TEA were purchased from Sigma-Aldrich GmbH, Austria. PNGase was obtained from Roche Diagnostics GmbH, Germany. Amiloride hydrochloride hydrate (Sigma-Aldrich GmbH, Austria) was used at a concentration of 10  $\mu$ M in order to block ENaC.

### **Statistical analysis**

Data represent the mean  $\pm$  S.E. unless otherwise stated; experiments were performed on three to seven batches of independently transfected cells in heterologous expression system. Statistical significance between different groups was determined using an unpaired, two-tailed Student's *t* test using GraphPad Prism version 3.02 (GraphPad Software, San Diego). Dose-response curves were plotted, and EC<sub>50</sub> values and Hill coefficients were determined using Microcal Origin 7.0. The activity of AP301 was expressed as a percentage of the paired amiloride response because of variability in hENaC expression between different batches of cultured cells. Amiloride was used at 10  $\mu$ M for  $\alpha\beta\gamma$ - and  $\delta\beta\gamma$ -hENaC in

MOL # 89409

HEK and CHO cells; these concentrations yielded greater than 95% hENaC inhibition. Only cells with clear amiloride response were included in data analysis. For whole-cell patch clamp experiments in RPMI-2650 cells amiloride-sensitive inward currents were evoked after trypsin application.

MOL # 89409

## RESULTS

### **AP301 activates amiloride-sensitive sodium current in HEK-293 cells transiently expressing hENaC**

Previously we showed that AP301 activates amiloride-sensitive current in A549 cells (Hazemi et al., 2010), a human lung adenocarcinoma cell line endogenously expressing ENaC. The A549 cell line is a widely accepted cell model of ENaC research (Lazrak et al., 2000). AP301 activates amiloride sensitive epithelial sodium channels in freshly isolated type II cells of rat, pig and dog (Tzotzos et al., 2013). Besides ENaC, A549 cells have other endogenously expressed cation channels like CNG channels; mRNA for CNG channels was detected in RT-PCR studies of A549 cells (Xu et al., 1999). CNG channels are also known to play a substantial role in alveolar liquid clearance (Wilkinson et al., 2011). Thus, to further characterize the ENaC activation effect of AP301 it was necessary to express hENaC heterologously (HEK-293 and CHO cells). A previous study has reported insignificant expression of  $\alpha$ - and  $\gamma$ -ENaC subunits in non-transfected HEK-293 cells (Ruffieux-Daidie et al., 2008). In accordance, we also found low amplitude transient leak sodium current in non-transfected HEK-293 cells.

To characterize effects on ENaC current, experiments were performed with  $\alpha\beta\gamma$ -hENaC transiently expressed in HEK-293 cells. Therefore, potential contributions from CNG channels were blocked with either 300  $\mu$ M L-cis-diltiazem (L-Cis) or 1 mM  $\text{Zn}^{2+}$ . Transfected cells showed a current amplitude of  $79.7 \pm 3.5$  pA before and  $75.98 \pm 2.8$  pA after the application of L-Cis (300 $\mu$ M) ( $p = 0.2239$ ,  $n=5$ ). Subsequent application of AP301 (120 nM) increased inward sodium current to  $1035.2 \pm 4.4$  pA ( $p<0.001$ ,  $n=5$ ), and final addition of amiloride (up to 100  $\mu$ M) blocked almost all AP301 induced current ( $26.7 \pm 3.2$  pA,  $n=5$ ). These data suggest that AP301 activation of hENaC is independent of L-Cis blocked channels (Fig. 1A). Next, HEK-293 cells transiently expressing hENaC were treated with 1 mM  $\text{Zn}^{2+}$ . These transfected cells showed a current amplitude of  $97.7 \pm 5.4$  pA in control and  $95.4 \pm 5.6$  pA in 1 mM  $\text{Zn}^{2+}$  treated cells ( $p=0.5324$ ,  $n=5$ ). Subsequent application of AP301 (120 nM) increased inward sodium current to  $549.2 \pm 4.1$  pA ( $p<0.001$ ,  $n=5$ ), and final

MOL # 89409

addition of amiloride (up to 100  $\mu$ M) blocked the AP301-induced current through ENaC ( $35.3 \pm 6.5$  pA) (Fig. 1B). Experiments indicating that L-Cis and  $Zn^{2+}$  do not alter AP301-induced currents were performed by adding L-Cis and  $Zn^{2+}$  after the application of AP301 ( $n=3$ ).

To further characterize that AP301 increases specifically sodium influx into the cell, ion substitution experiments were performed in both A549 and  $\alpha\beta\gamma$ -hENaC transfected HEK-293 cells. When sodium chloride in the bath solution was replaced with equimolar concentration of sodium aspartate to exclude  $Cl^-$  as charge carrier, AP301 increased inward current to the same extent as with NaCl in the bath solution ( $n=3$ ; data not shown). To confirm that AP301 activates cation conductance in HEK-293 cells transfected with  $\alpha\beta\gamma$ -hENaC, we studied the properties of channel currents using a bath solution containing the less permeant cation, NMDG-Cl, as the main charge carrier, instead of NaCl. With NaCl in the bath solution, HEK-293 cells transfected with  $\alpha\beta\gamma$ -hENaC showed a control current of  $114 \pm 4.6$  pA, whereas with NMDG-Cl in the bath solution HEK-293 cells transfected with  $\alpha\beta\gamma$ -hENaC showed a control current of  $8.5 \pm 9.9$  pA ( $p<0.001$ ). AP301 (120 nM) failed to activate inward currents in sodium free (NMDG-Cl) bath solution ( $8.6 \pm 3.4$  pA,  $n=9$ ), whereas application of AP301 (120 nM) increased inward current to  $987.4 \pm 6.1$  pA in experiments with NaCl as charge carrier ( $p<0.001$ ). AP301 failed to activate inward currents in sodium-free solutions, indicating that AP301 responses in sodium-replete solution were attributable to sodium influx (Fig. 1C). To further confirm that AP301 activates  $\alpha\beta\gamma$ -hENaC transfected in HEK-293 we used AICAR. Pre-incubation with AICAR of A549 (Tzotzos et al., 2013) or H441 cells (Albert et al., 2008) expressing ENaC endogeneously, blocked the amiloride sensitive sodium current. It has been shown that AICAR and associated activation of AMPK inhibits the constitutive activity of two amiloride-sensitive ENaC related channels in H441 cells by decreasing channel open probability. Whereas, no change in abundance of ENaC protein in the apical membrane of H441 cells after treatment with AICAR was detected (Albert et al., 2008). HEK-293 cells transfected with  $\alpha\beta\gamma$ -hENaC showed an inward control current of  $78.8 \pm 3.5$  pA. Pre-incubation of these transfected cells with 1 mM AICAR for 2h blocked inward current substantially ( $53.8 \pm 9.4$  pA,  $n=7$ ) ( $p<0.05$ ). Accordingly, AP301 (120 nM) was unable to

MOL # 89409

activate inward sodium current ( $55.1 \pm 8.4$  pA,  $n=7$ ). Subsequent application of amiloride (up to 100  $\mu$ M) blocked further inward current ( $11.6 \pm 6.0$  pA) (Fig. 1D). These data expand on our previous observations to show that AP301 is a novel and potent activator of hENaC.

### ***AP301 activates hENaC in a reversible manner***

Experiments were performed to characterize reversibility of the binding of AP301 on ENaC in A549 cells and heterologously expressed hENaC in HEK-293 cells. AP301 elicited a prompt response from ENaC to increase amiloride sensitive sodium current within 1-2 min. After steady-state was reached (5 min) subsequent application of control solution brought about a reversal of the current to control values within four pulses, indicating a fast dissociation of AP301 from ENaC (Fig. 2 A,B).

### ***Effects of AP301 and its congener AP318 on single channel current***

TNF- $\alpha$  and TIP-peptides 301 and 318 induced a marked, concentration-dependent increase of macroscopic Na<sup>+</sup> current through ENaC in A549 cells. To study the mechanism of this increase in current, effects of TNF- $\alpha$ , AP301 and the more potent TIP-peptide, AP318, on single channel current were examined in the cell-attached mode of the patch clamp technique. Experiments were performed at holding potentials of +60 and -60 mV. For single channel Na<sup>+</sup> current measurements, in all experiments 10 mM TEA was added to the pipette solution to block the potassium channel. TNF- $\alpha$ , AP301 and AP318 were added at EC<sub>50</sub> concentrations (8, 55 and 25 nM, respectively) to the pipette solution. The amplitude and open probability (Po) were calculated from all event histograms. In controls, Na<sup>+</sup> current with a conductivity of  $9.4 \pm 0.1$  pS ( $n=18$ ) was observed. This parameter was not significantly changed by TNF- $\alpha$  ( $9.8 \pm 0.1$  pS,  $n=10$ ), AP301 ( $9.7 \pm 0.1$  pS,  $n=7$ ) or AP318 ( $9.6 \pm 0.3$  pS,  $n=9$ ). When amiloride (10  $\mu$ M) was included in the pipette solution, no channel activity was seen ( $n=3$ ). In the cell-attached mode, TNF- $\alpha$ , AP301 and AP318 significantly increased Po of single channels without affecting the current amplitude (Table 1, Figure 3). Besides mean open time, also the number of bursts, and the duration of bursts were significantly increased

MOL # 89409

by TNF- $\alpha$  as well as AP301 and AP318 (Table 1). Accordingly, effects of TNF- $\alpha$ , AP301 and AP318 on macroscopic Na<sup>+</sup> current were confirmed by single channel current measurements.

TEA-sensitive K<sup>+</sup> current was measured with a conductivity of  $261 \pm 20$  pS (n=6). This estimated conductance is very close to the value of  $242 \pm 33$  pS reported for the TEA-sensitive Ca<sup>2+</sup>-activated K<sup>+</sup> channel in A549 cells (Ridge et al., 1997). Single channel parameters were not changed significantly by TNF- $\alpha$  or AP301 and AP318. This finding confirms the data obtained with whole-cell recordings (Hazemi et al. 2010).

### ***AP301 increases amiloride-sensitive current only in post-translationally modified hENaC***

It has been reported that ENaC is regulated with two unrelated pathways, one involving the ubiquitin system, and the other luminal serine proteases. ENaC can be activated by intracellular serine proteases and by exogenous application of trypsin when heterologously expressed in oocytes (Chraïbi et al., 1998; Diakov et al., 2008; Shi et al., 2013), and fibroblasts (Caldwell et al., 2004). Proteolytic cleavage of  $\alpha$ - and  $\gamma$ -ENaC subunits by furin and prostatic trypsin is necessary to obtain full channel activity from ENaC expressed in CHO cells (Hughey et al., 2007). ENaC is also regulated by sodium self-inhibition, which causes decreased inward sodium current. It was shown that ENaC activity could be increased by apical treatment with human neutrophil elastase (hNE) in a human airway epithelial cell line expressing ENaC endogenously (Caldwell et al., 2005).

To independently determine whether AP301 increases  $P_o$  of near-silent hENaC channels, experiments were performed with HNEC (RPMI-2650) cells. These cells have been shown to express ENaC which can be activated with hNE (Prulière-Escabasse et al., 2010). RPMI-2650 cells showed very little ( $52.0 \pm 3.5$  pA, n=18) inward current at -100 mV test pulses. Application of AP301 up to 240 nM induced a very low current ( $57.7 \pm 3.1$  pA, n=18), and final addition of amiloride inhibited this current ( $47.5 \pm 6.5$  pA, n=18) (Fig. 4 A, B). In contrast, when trypsin (100  $\mu$ g/ml) was applied, a transient increase in inward current was



MOL # 89409

seen which reached a steady state level after 4-5 pulses ( $76.2 \pm 3.8$  pA,  $n=11$ ). Subsequent application of AP301 (120 nM) showed a robust increase in inward sodium influx ( $662.1 \pm 4.2$  pA,  $n=11$   $p<0.001$ ). Final addition of amiloride blocked almost all of this AP301-induced current ( $43.9 \pm 3.8$  pA,  $n=11$ ) (Fig. 4C,D). These data indicate that AP301 activates proteolytically activated (cleaved) but not near silent (uncleaved) ENaC.

### ***Activation of hENaC in different cell lines with AP301***

HEK-293 and CHO cells are widely used model cell lines for the expression of foreign proteins. We have previously shown that AP301 increases amiloride-sensitive current in A549 cells expressing ENaC endogenously. The aim of this study was to characterize AP301 activation of hENaC in heterologous expression systems. To this end we transiently and stably expressed  $\alpha\beta\gamma$ -hENaC in HEK-293 and/or CHO cells. Dose response experiments were performed in whole cell configuration to investigate the amiloride block after AP301 activation. As shown in Fig. 5 A activation of hENaC with AP301 was similar in all three cell models with  $EC_{50}$  values in HEK-293 cells of  $54.7 \pm 2.24$  nM ( $n=7$ ), in CHO cells of  $58.1 \pm 1.9$  nM ( $n=9$ ) and in A549 cells of  $54.7 \pm 1.0$  nM ( $n=11$ ). In all these cell models a higher concentration of amiloride was needed to block the AP301-induced current than in the absence of AP301. As shown in Fig. 5 B a more than 2.5 fold higher ( $25.09 \pm 2.3$   $\mu$ M,  $n=7$ ) concentration of amiloride was required to block the AP301-induced current through hENaC compared to control current obtained in the absence of AP301 ( $9.8 \pm 1.2$   $\mu$ M,  $n=7$ ).

### ***hENaC subunit specific activation of AP301***

ENaC is a member of the degenerin family of non-voltage gated ion channels. In epithelial tissues the channel is composed of four homologous subunits ( $\alpha$ ,  $\beta$ ,  $\gamma$ ,  $\delta$ ) with 30-40% identity in their amino acid sequence (Canessa et al., 1994b, Althaus et al. 2011). It was shown that expression of  $\alpha$ -ENaC alone or in combination with either  $\beta$  or  $\gamma$ -ENaC is sufficient to make a conducting channel. In contrast, expression of  $\beta$ -ENaC or  $\gamma$ -ENaC alone in *Xenopus laevis* oocytes did not result in significant rENaC currents; co-expression of all

MOL # 89409

three subunits,  $\alpha$ ,  $\beta$  and  $\gamma$ , was needed for full channel activity (Canessa et al., 1994b; Snyder et al, 1994). It is widely accepted that all three subunits are glycosylated when expressed in a heterologous system (Staub et al., 1997) or in a cell-free translation assay, demonstrating that they share *in vitro* a common pattern of membrane insertion (Canessa et al., 1994a).

Studies were conducted to determine the subunit requirements of hENaC expressed in HEK-293 cells to activation by 120 nM AP301. In control experiments without addition of AP301, all hENaC subunits showed some transient amiloride-sensitive currents ( $\alpha$ -subunit:  $41.3 \pm 9.8$  pA,  $n=19$ ;  $\beta$ -subunit:  $15.6 \pm 8.5$  pA,  $n=19$ ;  $\gamma$ -subunit:  $19.1 \pm 7.3$  pA,  $n=19$ ;  $\delta$ -subunit:  $56.2 \pm 7.2$  pA,  $n=7$ ) when expressed alone or in dimeric combinations ( $\alpha\beta$ :  $33.1 \pm 5.4$  pA,  $n=21$ ;  $\alpha\gamma$ :  $39.2 \pm 7.9$  pA,  $n=21$ ;  $\beta\gamma$ :  $31.8 \pm 11.2$  pA,  $n=21$ ;  $\delta\beta$ :  $41.0 \pm 13.5$  pA,  $n=7$ ;  $\delta\gamma$ :  $34.5 \pm 10.0$  pA,  $n=7$ ), but these current amplitudes were significantly less than that of  $\alpha\beta\gamma$ -hENaC subunits ( $93.2 \pm 5.5$  pA,  $n=27$ ;  $p<0.001$ ) or  $\delta\beta\gamma$ -ENaC subunits triplets ( $117.2 \pm 6.9$  pA,  $n=7$ ;  $p<0.001$ ). AP301 treatment of HEK-293 cells expressing these same subunit combinations showed that, although some response ( $p<0.001$  compared to  $\alpha$ -subunit alone) may be elicited from cells co-expressing  $\alpha\beta$ -,  $\alpha\gamma$ -,  $\delta\beta$ - and  $\delta\gamma$ -subunits ( $316.0 \pm 1.8$  pA,  $452.0 \pm 2.0$  pA,  $291.8 \pm 7.2$  and  $441.5 \pm 11.7$  pA, respectively) three WT  $\alpha\beta\gamma$ -hENaC or  $\delta\beta\gamma$ -ENaC subunits are necessary to elicit a rapid and robust response to AP301 ( $953.2 \pm 3.4$  pA,  $n=21$  and  $1002.1 \pm 9.1$ , respectively) (Fig 6 A,B).

### ***Effect of deglycosylation on activation of amiloride-sensitive sodium current by TNF- $\alpha$ and AP301 in A549 cells***

The effect of AP301 (120 nM) was studied in cell-excised multi-channel inside-out and outside-out patches of A549 cells. Mean values of total currents are shown in Fig 7 A. In control, outside-out patches' current amplitude of  $5.1 \pm 1.3$  pA ( $n=17$ ) was significantly increased to  $15.3 \pm 0.9$  pA ( $n=17$ ,  $p<0.001$ ) with 120 nM AP301 in the bath solution. In contrast, inside-out patch clamp configuration did not yield increased total inward current (control:  $4.9 \pm 2.3$  pA, 120 nM AP301:  $4.8 \pm 5.7$  pA,  $n=13$ ) when AP301 was applied to the

MOL # 89409

bath solution (Fig. 7A). These data suggest that activation of hENaC by AP301 requires its interaction with the extracellular loop region of ENaC.

To further characterize this effect, deglycosylation of the extracellular loops of ENaC was performed with endoglycosidase. A549 cells showed a current amplitude of  $90.3 \pm 3.5$  pA before and  $84.0 \pm 6.1$  pA ( $n=17$ ) after the treatment with 100 units PNGase. Subsequent application of 120 nM AP301 induced no increase in inward sodium current in PNGase treated cells ( $85.5 \pm 2.9$  pA,  $n=17$ ) whereas the same concentration of AP301 has yielded a 10 fold higher inward current ( $1073.3 \pm 5.4$  pA,  $n=14$ ,  $p<0.001$ ) in non-PNGase treated cells. Final addition of amiloride has blocked the AP301-induced current (Fig 7 B). In addition to whole-cell recordings, deglycosylation of the A549 cell membrane was performed with PNGase F also in single channel patches in the cell-attached mode. In this case, the enzyme was added to the pipette solution. Single channel studies confirmed the effect of deglycosylation with PNGase F found in whole-cell recordings. In PNGase F-untreated cell membranes,  $P_o$  was significantly increased by TNF- $\alpha$  and TIP-peptides (control:  $P_o$   $0.09 \pm 0.02$ , conductivity  $9.6 \pm 0.2$  pS,  $n=10$ ; TNF- $\alpha$ :  $P_o$   $0.77 \pm 0.08$ , conductivity  $9.8 \pm 0.1$  pS,  $n=10$ ; AP301:  $P_o$   $0.69 \pm 0.05$ , conductivity  $9.7 \pm 0.1$  pS,  $n=7$ ; AP318:  $P_o$   $0.78 \pm 0.05$ , conductivity  $9.6 \pm 0.3$  pS) whereas after deglycosylation no effect of TNF- $\alpha$  and TIP peptides on  $P_o$  and conductivity could be observed (control:  $P_o$   $0.09 \pm 0.01$ ,  $9.6 \pm 0.2$  pS; TNF- $\alpha$ :  $P_o$   $0.10 \pm 0.03$ ,  $9.6 \pm 0.4$  pS,  $n=4$ ; AP301:  $P_o$   $0.09 \pm 0.02$ ,  $9.7 \pm 0.4$  pS,  $n=3$ ; AP318:  $P_o$   $0.10 \pm 0.02$ ,  $9.6 \pm 0.4$  pS,  $n=3$ ), indicating the participation of sugar moieties of the cell membrane in binding of TIP-peptides.

To independently characterize the effect of AP301 in deglycosylated loop(s), experiments were next performed in a heterologous expression system. For this purpose HEK-293 cells were transfected with  $\alpha\beta\gamma$ -hENaC. In these experimental settings transfected HEK-293 cells showed a current of  $79.2 \pm 4.0$  pA ( $n=21$ ) before and  $68.3 \pm 5.1$  pA ( $n=21$ ) after the treatment with PNGase. Subsequent application of 120 nM AP301 induced no increase in inward sodium current in PNGase treated cells ( $67.3 \pm 4.2$  pA,  $n=19$ ) whereas the same concentration of AP301 has yielded a 10 fold higher current ( $1086.2 \pm 7.4$  pA,  $n=19$ ,

MOL # 89409

$p < 0.001$ ) in non-PNGase treated cells. Final addition of amiloride has blocked the AP301-induced current (Fig 7 C). To rule out the possible activation of transient leak current with AP301, experiments were performed in non-transfected HEK-293 cells in control and after PNGase enzyme treatment. Non-transfected cells showed a transient leak current of  $1.1 \pm 6.0$  pA ( $n=31$ ) before and  $11.1 \pm 5.0$  pA ( $n=31$ ) after the treatment with PNGase. Subsequent application of 120 nM AP301 showed no increase in inward sodium current in PNGase treated ( $14.5 \pm 6.4$  pA,  $n=11$ ) as well as non-PNGase treated cells ( $14.5 \pm 5.9$  pA,  $n=11$ ). Final addition of amiloride has shown a minimal current block (Fig 7 D). Thus, our data suggest that binding of AP301 to a specific binding site of ENaC requires precedent interaction with glycosylated extracellular loop(s) in both endogenously and heterologously expressed ENaC.

## DISCUSSION

Alveolar fluid clearance (AFC) is regulated by cation and anion channels as well as ion transporters. Cation channels include ENaC (Folkesson and Matthay, 2006; Berthiaume and Matthay, 2007; Eaton et al., 2009), CNG (Wilkinson et al., 2011) and  $K^+$  channels (Bardou et al., 2009). Chloride channels that contribute to AFC enclose CFTR (Lazrak et al., 2011, Solymosi et al., 2013) and other  $Cl^-$  channels such as the GABA<sub>A</sub> receptor (Jin et al., 2006), voltage-gated  $Cl^-$  channels, CLC5 and CLC2, and a basolaterally located  $Cl^-$  channel (Berger et al., 2010; Hollenhorst et al., 2011). In previous studies and the present study we could exclude CNG channels (Tzotzos et al. 2013) and  $K^+$  channels (Hazemi et al. 2013) as main targets for our lead compound AP301. Furthermore, in the present study we could also exclude chloride channels as a target for AP301, because upon replacement of sodium chloride in the bath solution with equimolar concentration of sodium aspartate, AP301 still increased inward current to the same extent. Based on these findings we suggest ENaC as the main target for TIP peptides, and thus further characterized the effects of AP301 on ENaC.

MOL # 89409

To our knowledge only a few ENaC activators are known. One, S3969, a small molecule opener of ENaC, increases hENaC  $P_o$  in a  $\beta$ -subunit dependent manner in heterologous expression system and second, Lipoxin A4, increases  $\alpha$  and  $\gamma$ -ENaC protein expression and  $\text{Na}^+$ - $\text{K}^+$ -ATPase activity in an animal model (Lu et al., 2009, Wang et al., 2013). We have previously shown that AP301, a TNF- $\alpha$  lectin like domain derived peptide, can increase amiloride sensitive current in A549 cells (Hazemi et al., 2010) as well as in freshly isolated type II alveolar epithelial cells from different species (Tzotzos et al., 2013); in all these cell types ENaC is expressed endogenously.

In the present study we have shown that a TNF- $\alpha$  lectin like domain derived peptide activates inward sodium influx through ENaC in a heterologous expression system.

### ***Effects of TIP peptides on single channel current kinetics***

Macroscopic current depends on the number, single channel current and  $P_o$  of functional channels in the plasma membrane. TIP peptides could activate ENaC by increasing one or more of these parameters. The observed immediate stimulatory effect of AP301 points rather to a direct effect on the channel kinetics in the plasma membrane than to an increase of the number of channels by promoting vesicular trafficking of newly synthesized channels from an intracellular pool to the cell surface, a process which would require tens of minutes (Carattino et al., 2003). The former mechanism was reported for S3969, a small molecule activator of ENaC in the micromolar range (Lu et al., 2008). Indeed, our results show that AP301 and AP318 significantly increased open time, number and duration of bursts in single channel current without affecting single channel current amplitude. Although our data, derived from macroscopic and single channel recordings, indicate that AP301 and AP318 activate hENaC by increasing  $P_o$ , an additional effect on the expression of ENaC still has to be verified. Moreover, how AP301 increases open probability of ENaC remains to be elucidated.

### ***Specificity of ENaC activation***

MOL # 89409

Previous studies led to the conclusion that it is unlikely that HEK-293 cells produce endogenous ENaC (Ruffieux-Daidie et al., 2008) since mRNA encoding  $\alpha$ -,  $\beta$ - and  $\gamma$ -ENaC was not detected in real time PCR experiments with non-transfected HEK-293 cells; nevertheless the same researchers observed endogenous cross reacting proteins to antibodies of  $\alpha$ - and  $\gamma$ -ENaC in Western blots of non-transfected HEK-293 cells. We also found a small sodium leak current in non-transfected HEK-293 cells. Consequently, contribution of any non-selective cation channel (Qiu et al., 2000; Xu et al., 1999) and potential contribution of CNG channels were blocked with L-Cis or  $\text{Zn}^{2+}$  as these channels also conduct amiloride sensitive current. The concentration of amiloride required to bring about 50% inhibition of CNG channels ( $\text{IC}_{50}$ , the half maximum inhibitory concentration) is 39-125  $\mu\text{M}$  (Xu et al., 1999), while for the moderately selective ENaC described in A549 cells (Lazrak, 2000) the  $\text{IC}_{50}$  for amiloride is 10  $\mu\text{M}$ , and for highly selective (HSC) and non-selective (NSC) ENaC in H441 cells (Albert et al., 2008) lower  $\text{IC}_{50}$  concentrations of 1  $\mu\text{M}$  and 10  $\mu\text{M}$ , respectively, are observed. In HEK-293 cells expressing  $\alpha\beta\gamma$ -hENaC, application of AP301 showed increased inward sodium current following the treatment of L-Cis and  $\text{Zn}^{2+}$ . To block this AP301-induced current, higher amiloride concentrations ( $\text{IC}_{50} = 25 \mu\text{M}$ ) were necessary than in control ( $\text{IC}_{50} = 9.8 \mu\text{M}$ ). Increased amiloride sensitive current, following addition of AP301 subsequent to L-Cis or  $\text{Zn}^{2+}$ , in HEK-293 cells transfected with  $\alpha\beta\gamma$ -hENaC, suggests that AP301 interacts with ENaC as its first target. This finding is supported by the fact that ENaC could not be activated by AP301 either when NMDG replaced sodium ions as charge carrier or following pre-treatment of the cells with AICAR, which we solely used as a molecular tool to block amiloride sensitive sodium current. This blockade is reported to be caused by activation of AMP-activated protein kinase, but did not increase cell surface expression of ENaC proteins (Albert et al., 2008).

The maximal stimulatory effect of AP301 on hENaC function in human cell lines is acute and current rapidly returns to baseline following AP301 washout. Reversible ENaC activation suggests that AP301 interacts non-covalently with ENaC channels.

MOL # 89409

### ***Subunit requirements for maximal current activation***

Maximum activation with AP301 was observed when the pore-forming ENaC subunits,  $\alpha$  or  $\delta$ , were co-expressed with  $\beta$ - and  $\gamma$ -subunits. For pairwise combinations of subunits co-expressed heterologously, a significant enhancement of current by AP301 was seen with the  $\alpha\beta$ ,  $\alpha\gamma$ ,  $\delta\beta$  and  $\delta\gamma$  subunit combinations, but not with the  $\beta\gamma$  combination. These findings are in contrast to those of Lu et al. (2008), who showed a current activation with S3969 which was observed only in oocytes co-expressing  $\alpha$ -,  $\beta$ -, and  $\gamma$ -ENaC, but not in cells expressing any of the possible pairwise subunit combinations. The reason why  $\beta\gamma$ -ENaC-subunit combination did not show an effect with AP301 is unclear; possible explanations are the absence of co-expression of the  $\alpha$ -subunit that has been previously shown to be required for expression of maximal channel activity at the plasma membrane (Canessa et al., 1994b) and that specific binding site(s) might be located at the  $\alpha$ - and  $\delta$ -subunit. Our data suggest that the binding pocket for AP301 activation of ENaC is only optimally formed upon co-expression of pore-forming  $\alpha$ - or  $\delta$ -subunit together with  $\beta\gamma$ -subunits.

### ***Effect on proteolytically cleaved or quiescent ENaC***

Our experiments indicate that the amiloride sensitive  $\text{Na}^+$  current enhancing effect of AP301 requires ENaC which has been proteolytically cleaved and released from  $\text{Na}^+$  dependent self-inhibition. The majority of channels in the RPMI-2650 cell membrane are closed or in a quiescent, non-conducting state (Prulière-Escabasse et al., 2010). Non-conducting or quiescent ENaC may be poorly accessible to AP301. Following transition from closed to open state after trypsin treatment, AP301 may interact with ENaC to stabilize an open conformation thereby inducing longer openings of the channel. The  $\text{EC}_{50}$  values in the three cell models (A549,  $\alpha\beta\gamma$ -ENaC expressed in HEK-293,  $\alpha\beta\gamma$ -ENaC expressed in CHO) are almost the same, indicating that AP301 activates ENaC in a similar manner. Before pre-incubation with low concentration of  $\text{Na}^+$  solution to remove sodium dependent self-inhibition, HEK-293 cells transfected with  $\alpha\beta\gamma$ -ENaC showed small currents with AP301. Only after removal of sodium dependent self-inhibition, AP301 was able to activate inward sodium

MOL # 89409

current. In contrast, ENaC produced in CHO cells, co-expressing  $\alpha$ ,  $\beta$  and  $\gamma$ -ENaC subunits, a larger initial open probability owing to endogenous proteolysis (Hughey et al., 2004b). In these cells AP301 elicited immediate activation of inward current. Similarly, A549 cells showed larger control currents and robust AP301 response. These data indicate that activation by AP301 requires proteolytically processed channels. In addition, these findings provide indirect support for the therapeutic potential of AP301 in ALC in pulmonary oedema. Increased concentrations of proteases in combination with decreased concentrations of the naturally occurring protease inhibitor  $\alpha$ -1-AP in the lungs are characteristic pathophysiological features in patients with lung oedema and ARDS; consequently alveolar ENaC in oedema patients is likely to be proteolytically cleaved (Hunninghake et al., 1979). This would ultimately facilitate access of AP301 to the channel. Furthermore, inability of AP301 to activate near silent ENaC suggests that AP301 is unable to release ENaC from a quiescent state or from sodium self-inhibition in the manner of serine proteases (Chraïbi et al., 1998; Caldwell et al., 2004; Sheng et al., 2006). These data are in contrast to the findings of Lu et al. (2008), who reported that hENaC activation by S3969 does not require cleavage by furin proteases.

### ***Requirement of glycosylated ENaC for interaction***

Our findings that AP301 activation of hENaC specifically required glycosylated extracellular domains of ENaC to enable binding to the so far unidentified specific binding site of TIP peptides are based on the following results: In inside-out multi-channel patches AP301 showed no activation of sodium current, while in outside-out multi-channel patches AP301 induced inward current increase when the test compound was applied to the bath solution. Furthermore, deglycosylation of cell membranes abolished inward current activation by AP301. This was demonstrated in whole-cell recordings and in single channel experiments in both endogenously as well as heterologously expressed hENaC. Recent docking and molecular dynamics simulation experiments have indicated that the TIP peptide AP301 represents a partial binding motif for chitobiose (Dulebo et al., 2012). By definition,



MOL # 89409

lectins bind to glycans, and our data clearly show that glycosylation of ENaC is necessary for activation with AP301. To note, it has been shown previously that removing glycosylation sites did not affect the conductance of ENaC indicating that deglycosylation has no effect on channel function (Snyder et al., 1994).

In all tested cell models a higher concentration of amiloride was needed to block the AP301-induced current than in the absence of AP301. Amiloride potency shift after AP301 treatment is still an unresolved phenomenon. We hypothesize that more than one mechanism may be involved. Mutagenesis studies have identified residues in the outer pore entrance that are critical for ENaC block by amiloride (Kellenberger et al., 2003). Thus, docking of AP301 to a glycosylation site in the vicinity of these residues could be aggravated. Preliminary data from mutagenesis studies further corroborate our findings (data not shown).

To conclude, we have shown that the TNF- $\alpha$  lectin like domain derived peptide, AP301, i) specifically targets endogenously and heterologously expressed ENaC, ii) activates proteolytically processed ENaC in a reversible manner, iii) requires the pore-forming  $\alpha$ - or  $\delta$ -subunit, co-expressed with  $\beta\gamma$ -subunits, for maximal activity, and iv) requires glycosylated extracellular domains of ENaC to enable binding to an unidentified specific binding site.

MOL # 89409

## **ACKNOWLEDGEMENTS**

The authors thank Drs. Deborah L Baines, Peter M Snyder and Mike Althaus for providing hENaC expression cDNA.

MOL # 89409

## **AUTHORSHIP CONTRIBUTIONS**

Participated in research design: Shabbir, Lucas, Lemmens-Gruber

Conducted experiments: Shabbir, Scherbaum-Hazemi

Contributed new reagents or analytic tools: Tzotzos, Fischer B., Fischer H., Pietschmann

Performed data analysis: Shabbir, Scherbaum-Hazemi, Lemmens-Gruber

Wrote or contributed to the writing of the manuscript: Shabbir, Tzotzos, Lemmens-Gruber

MOL # 89409

## REFERENCES

- Adams CM, Snyder PM, Welsh MJ (1997) Interactions between subunits of the human epithelial sodium channel. *J Biol Chem* **272**: 27295-27300.
- Albert AP, Woollhead AM, Mace OJ, Baines DL (2008) AICAR decreases the activity of two distinct amiloride-sensitive Na<sup>+</sup>-permeable channels in H441 human lung epithelial cell monolayers. *Am J Physiol Lung Cell Mol Physiol* **295**: L837-848.
- Althaus M, Clauss WG, Fronius M (2011) Amiloride-sensitive sodium channels and pulmonary edema. *Pulm Med* **2011**:830320-830328.
- Bardou O, Trinh NT, Brochiero E (2009) Molecular diversity and function of K<sup>+</sup> channels in airway and alveolar epithelial cells. *Am J Physiol Lung Cell Mol Physiol* **296**:L145-155.
- Benos DJ (1982) Amiloride: a molecular probe of sodium transport in tissues and cells. *Am J Physiol* **242**: C131-145.
- Berger J, Richter K, Clauss WG, Fronius M (2011) Evidence for basolateral Cl<sup>-</sup> channels as modulators of apical Cl<sup>-</sup> secretion in pulmonary epithelia of *Xenopus laevis*. *Am J Physiol Regul Integr Comp Physiol* **300**: R616-623.
- Berthiaume Y, Matthay MA (2007) Alveolar edema fluid clearance and acute lung injury. *Respir Physiol Neurobiol* **159**: 350-359.
- Braun C, Hamacher J, Morel DR, Wendel A, Lucas R (2005) Dichotomal role of TNF in experimental pulmonary edema reabsorption. *J Immunol* **175**: 3402-3408.
- Caldwell RA, Boucher RC, Stutts MJ (2004) Serine protease activation of near-silent epithelial Na<sup>+</sup> channels. *Am J Physiol Cell Physiol* **286**:C190-194.
- Caldwell RA, Boucher RC, Stutts MJ (2004) Neutrophil elastase activates near-silent epithelial Na<sup>+</sup> channels and increases airway epithelial Na<sup>+</sup> transport. *Am J Physiol Lung Cell Mol Physiol* **288**:L813-819.
- Canessa CM, Merillat AM, Rossier BC (1994a) Membrane topology of the epithelial sodium channel in intact cells. *Am J Physiol* **267**:C1682-1690.

MOL # 89409

Canessa CM, Schild L, Buell G, Thorens B, Gautschi I, Horisberger JD, Rossier BC (1994b) Amiloride-sensitive epithelial Na<sup>+</sup> channel is made of three homologous subunits. *Nature* **367**:463-467.

Carattino MD, Hill WG, Kleyman TR (2003) Arachidonic acid regulates surface expression of epithelial sodium channels. *J Biol Chem* **278**:36202-36213.

Chraïbi A, Vallet V, Firsov D, Hess SK, Horisberger JD (1998) Protease modulation of the activity of the epithelial sodium channel expressed in *Xenopus* oocytes. *J Gen Physiol* **111**:127-138.

Chraïbi A, Horisberger JD (1999) Stimulation of epithelial sodium channel activity by the sulfonylurea glibenclamide. *J Pharmacol Exp Ther* **290**:341-347.

Diakov A, Bera K, Mokrushina M, Krueger B, Korbmacher C (2008) Cleavage in the {gamma}-subunit of the epithelial sodium channel (ENaC) plays an important role in the proteolytic activation of near-silent channels. *J Physiol* **586**:4587-4608.

Dulebo A, Ettrich R, Lucas R, Kaftan D (2012) A computational study of the oligosaccharide binding sites in the lectin-like domain of Tumor Necrosis Factor and the TNF-derived TIP peptide. *Curr Pharm Des* **18**:4236-4243.

Eaton DC, Helms MN, Koval M, Bao HF, Jain L (2009) The contribution of epithelial sodium channels to alveolar function in health and disease. *Annu Rev Physiol* **71**: 403-423.

Elia N, Tapponnier M, Matthay MA, Hamacher J, Pache JC, Brundler MA, Totsch M, De Baetselier P, Fransen L, Fukuda N, Morel DR, Lucas R (2003) Functional identification of the alveolar edema reabsorption activity of murine tumor necrosis factor-alpha. *Am J Respir Crit Care Med* **168**:1043-1050.

Folkesson HG, Matthay MA (2006) Alveolar epithelial ion and fluid transport: recent progress. *Am J Respir Cell Mol Biol* **35**:10-19.

Fukuda N, Jayr C, Lazrak A, Wang Y, Lucas R, Matalon S, Matthay MA (2001) Mechanisms of TNF-alpha stimulation of amiloride-sensitive sodium transport across alveolar epithelium. *Am J Physiol Lung Cell Mol Physiol* **280**:L1258-1265.

MOL # 89409

- Gaillard EA, Kota P, Gentzsch M, Dokholyan NV, Stutts MJ, Tarran R (2010) Regulation of the epithelial Na<sup>+</sup> channel and airway surface liquid volume by serine proteases. *Pflugers Arch* **460**: 1-17.
- Hamacher J, Stammberger U, Roux J, Kumar S, Yang G, Xiong C, Schmid RA, Fakin RM, Chakraborty T, Hossain HM, Pittet JF, Wendel A, Black SM, Lucas R (2010) The lectin-like domain of tumor necrosis factor improves lung function after rat lung transplantation--potential role for a reduction in reactive oxygen species generation. *Crit Care Med* **38**:871-878.
- Hartmann EK, Boehme S, Duenges B, Bentley A, Klein KU, Kwiecien R, Shi C, Szczyrba M, David M, Markstaller K (2013) An inhaled tumor necrosis factor-alpha-derived TIP peptide improves the pulmonary function in experimental lung injury. *Acta Anaesthesiol Scand* **57**:334-341.
- Hazemi P, Tzotzos SJ, Fischer B, Andavan GS, Fischer H, Pietschmann H, Lucas R, Lemmens-Gruber R (2010) Essential structural features of TNF-alpha lectin-like domain derived peptides for activation of amiloride-sensitive sodium current in A549 cells. *J Med Chem* **53**:8021-8029.
- Hirsh AJ, Molino BF, Zhang J, Astakhova N, Geiss WB, Sargent BJ, Swenson BD, Usyatinsky A, Wyle MJ, Boucher RC, Smith RT, Zamurs A, Johnson MR (2006) Design, synthesis, and structure-activity relationships of novel 2-substituted pyrazinoylguanidine epithelial sodium channel blockers: drugs for cystic fibrosis and chronic bronchitis. *J Med Chem* **49**:4098-4115.
- Hollenhorst MI, Richter K, Fronius M (2011) Ion transport by pulmonary epithelia. *J Biomed Biotechnol* **2011**:174306-174339.
- Hribar M, Bloc A, van der Goot FG, Fransen L, De Baetselier P, Grau GE, Bluethmann H, Matthay MA, Dunant Y, Pugin J, Lucas R (1999) The lectin-like domain of tumor necrosis

MOL # 89409

factor- $\alpha$  increases membrane conductance in microvascular endothelial cells and peritoneal macrophages. *Eur J Immunol* **29**:3105-3111.

Hughey RP, Mueller GM, Bruns JB, Kinlough CL, Poland PA, Harkleroad KL, Carattino MD, Kleyman TR (2003) Maturation of the epithelial Na<sup>+</sup> channel involves proteolytic processing of the  $\alpha$ - and  $\gamma$ -subunits. *J Biol Chem* **278**:37073-37082.

Hughey RP, Bruns JB, Kinlough CL, Kleyman TR (2004a) Distinct pools of epithelial sodium channels are expressed at the plasma membrane. *J Biol Chem* **279**:48491-48494.

Hughey RP, Bruns JB, Kinlough CL, Harkleroad KL, Tong Q, Carattino MD, Johnson JP, Stockand JD, Kleyman TR (2004b) Epithelial sodium channels are activated by furin-dependent proteolysis. *J Biol Chem* **279**: 18111-18114.

Hughey RP, Kleyman TR (2007) Functional cross talk between ENaC and pendrin. *Am J Physiol Renal Physiol* **293**: F1439-1440.

Hunninghake GW, Gadek JE, Kawanami O, Ferrans VJ, Crystal RG (1979) Inflammatory and immune processes in the human lung in health and disease: evaluation by bronchoalveolar lavage. *Am J Pathol* **97**:149-206.

Jin N, Kolliputi N, Gou D, Weng T, Liu L (2006) A novel function of ionotropic  $\gamma$ -aminobutyric acid receptors involving alveolar fluid homeostasis. *J Biol Chem* **281**: 36012-36020.

Johnson MD, Bao HF, Helms MN, Chen XJ, Tigue Z, Jain L, Dobbs LG, Eaton DC (2006) Functional ion channels in pulmonary alveolar type I cells support a role for type I cells in lung ion transport. *Proc Natl Acad Sci U S A* **103**:4964-4969.

Jovov B, Berdiev BK, Fuller CM, Ji HL, Benos DJ (2002) The serine protease trypsin cleaves C termini of  $\beta$ - and  $\gamma$ -subunits of epithelial Na<sup>+</sup> channels. *J Biol Chem* **277**:4134-4140.

Kleyman TR, Carattino MD, Hughey RP (2009) ENaC at the cutting edge: regulation of epithelial sodium channels by proteases. *J Biol Chem* **284**:20447-20451.

MOL # 89409

- Lazrak A, Samanta A, Matalon S (2000) Biophysical properties and molecular characterization of amiloride-sensitive sodium channels in A549 cells. *Am J Physiol Lung Cell Mol Physiol* **278**:L848-857.
- Lazrak A, Jurkuvenaite A, Chen L, Keeling KM, Collawn JF, Bedwell DM, Matalon S (2011) Enhancement of alveolar epithelial sodium channel activity with decreased cystic fibrosis transmembrane conductance regulator expression in mouse lung. *Am J Physiol Lung Cell Mol Physiol* **301**:L557-567.
- Lu M, Echeverri F, Kalabat D, Laita B, Dahan DS, Smith RD, Xu H, Staszewski L, Yamamoto J, Ling J, Hwang N, Kimmich R, Li P, Patron E, Keung W, Patron A, Moyer BD(2008) Small molecule activator of the human epithelial sodium channel. *J Biol Chem* **283**: 11981-11994.
- Lucas R, Magez S, De Leys R,Fransen L, Scheerlinck JP, Rampelberg M, Sablon E, De Baetselier P(1994) Mapping the lectin-like activity of tumor necrosis factor. *Science* **263**:814-817.
- Matthay MA, Robriquet L, Fang X(2005) Alveolar epithelium: role in lung fluid balance and acute lung injury. *Proc Am Thorac Soc* **2**:206-213.
- McDonald FJ, Snyder PM, McCray PB Jr, Welsh MJ (1994) Cloning, expression, and tissue distribution of a human amiloride-sensitive Na<sup>+</sup> channel. *Am J Physiol* **266**:L728-L734.
- Mutlu GM, Sznajder JI (2005) Mechanisms of pulmonary edema clearance. *Am J Physiol Lung Cell Mol Physiol* **289**:L685-695.
- Prulière-Escabasse V, Clerici C, Vuagniaux G,Coste A,Escudier E, Planès C (2010) Effect of neutrophil elastase and its inhibitor EPI-hNE4 on transepithelial sodium transport across normal and cystic fibrosis human nasal epithelial cells. *Respir Res* **11**:141-155.
- Qiu W, Laheri A, Leung S, Guggino SE (2000) Hormones increase mRNA of cyclic-nucleotide-gated cationchannelsin airway epithelia. *Pflugers Arch* **441**: 69-77.



MOL # 89409

Ruffieux-Daidie D, Poirot O, Boulkroun S, Verrey F, Kellenberger S, Staub O (2008)

Deubiquitylation regulates activation and proteolytic cleavage of ENaC. *J Am Soc Nephrol* **19**:2170-2180.

Schnizler M, Berk A, Clauss W (2003) Sensitivity of oocyte-expressed epithelial Na<sup>+</sup> channel to glibenclamide. *Biochim Biophys Acta* **1609**: 170-176.

Sheng S, Carattino MD, Bruns JB, Hughey RP, Kleyman TR (2006) Furin cleavage activates the epithelial Na<sup>+</sup> channel by relieving Na<sup>+</sup> self-inhibition. *Am J Physiol Renal Physiol* **290**:F1488-1496.

Shi S, Carattino MD, Hughey RP, Kleyman TR (2013) ENaC regulation by proteases and shear stress. *Curr Mol Pharmacol* **6**:28-34.

Snyder PM, McDonald FJ, Stokes JB, Welsh MJ (1994) Membrane topology of the amiloride-sensitive epithelial sodium channel. *J Biol Chem* **269**:24379-24383.

Solymosi EA, Kaestle-Gembardt SM, Vadász I, Wang L, Neye N, Chupin CJ, Rozowsky S, Ruehl R, Tabuchi A, Schulz H, Kapus A, Morty RE, Kuebler WM (2013) Chloride transport-driven alveolar fluid secretion is a major contributor to cardiogenic lung edema. *Proc Natl Acad Sci U S A* **110**:E2308-2316.

Staub O, Gautschi I, Ishikawa T, Breitschopf K, Ciechanover A, Schild L, Rotin D (1997) Regulation of stability and function of the epithelial Na<sup>+</sup> channel (ENaC) by ubiquitination. *EMBO J* **16**:6325-6336.

Tzotzos S, Fischer B, Fischer H, Pietschmann H, Lucas R, Dupre G, Lemmens-Gruber R, Hazemi P, Prymaka V, Shabbir W (2013) AP301, a synthetic peptide mimicking the lectin-like domain of TNF, enhances amiloride-sensitive Na<sup>(+)</sup> current in primary dog, pig and rat alveolar type II cells. *Pulm Pharmacol Ther* **26**:356-363.

Vadasz I, Schermuly RT, Ghofrani HA, Rummel S, Wehner S, Muhldorfer I, Schafer KP, Seeger W, Morty RE, Grimminger F, Weissmann N (2008) The lectin-like domain of tumor necrosis factor- $\alpha$  improves alveolar fluid balance in injured isolated rabbit lungs. *Crit Care Med* **36**:1543-1550.

MOL # 89409

Ware LB, Matthay MA (2001) Alveolar fluid clearance is impaired in the majority of patients with acute lung injury and the acute respiratory distress syndrome. *Am J Respir Crit Care Med* **163**:1376-1383.

Wilkinson WJ, Benjamin AR, De Proost I, Orogo-Wenn MC, Yamazaki Y, Staub O, Morita T, Adriaensen D, Riccardi D, Walters DV, Kemp PJ (2011) Alveolar epithelial CNGA1 channels mediate cGMP-stimulated, amiloride-insensitive, lung liquid absorption. *Pflugers Arch* **462**:267-279.

Xu W, Leung S, Wright J, Guggino SE (1999) Expression of cyclic nucleotide-gated cation channels in airway epithelial cells. *J Membr Biol* **171**: 117-126.

MOL # 89409

## FOOTNOTES

\*

W.S. P.H. received financial support by the Austrian Research Promotion Agency (FFG)

To whom correspondence should be addressed: Waheed Shabbir, Department of  
Pharmacology and Toxicology, University of Vienna, Althanstrasse 14, A-1090 Vienna,  
Austria

Phone: +43 1 4277 55309. FAX: +43 1 4277 9553. Email: [waheed.shabbir@univie.ac.at](mailto:waheed.shabbir@univie.ac.at)

MOL # 89409

## FIGURE LEGENDS

### Figure 1

#### **AP301 selectively activates $\alpha\beta\gamma$ -hENaC expressed in HEK-293 cells.**

A, mean values of inward currents during control phase, following sequential addition of L-cis-diltiazem (300  $\mu$ M), AP301 (120 nM) and final addition of amiloride (up to 100  $\mu$ M) to the bath solution (n =5). Cells were patched in the whole cell mode; inward current was elicited at -100 mV. B, mean values of inward currents during control phase, following sequential addition of  $Zn^{2+}$  (1 mM), AP301 (120 nM) and final addition of amiloride (up to 100  $\mu$ M) to the bath solution (n=5). C, mean values of AP301 (120 nM) activated inward current in sodium-replete solution ( $Na^+$ ), but not in sodium-free solution (NMDG) (n=9). D, mean values of AP301 (120 nM) induced current following treatment with AICAR (1 mM for 2 h); subsequent treatment with amiloride (up to 100  $\mu$ M) further inhibited inward sodium current (n=7).

\*\*\*,  $p < 0.001$  compared with control as determined by t test.

### Figure 2

#### **Reversibility of AP301-induced ENaC current activating effect in HEK-293 cells.**

A, representative whole-cell patch clamp recordings. Cells were patched in the whole cell mode; inward current was elicited at -100 mV. Steady state phase indicates steady state of AP301 activation. Wash-out pulses indicate returning of ENaC to baseline level after AP301 removal. B, AP301 (120 nM) induced inward current activation of  $\alpha\beta\gamma$ -hENaC transiently expressed in HEK cells. AP301 (120 nM) was applied to the bath solution until wash-in steady state phase (5 min). Subsequent perfusion with bath solution removed (washed-out) AP301 and current was returned to normal (control) level (n=3). Mean values  $\pm$  S.E. of 3 experiments are shown.

MOL # 89409

### Figure 3

#### Original recordings from a cell-attached patch of an A549 cell.

The A549 cell patch was clamped at a holding potential of -60 mV during control (left panel) and in presence of AP301 (right panel). Dashed lines indicate the closed state of the channel (C), and dotted lines indicate the open state (O, downward deflections). The recordings clearly indicate the longer duration of single channel openings with AP301.

### Figure 4

#### AP301 induced amiloride-sensitive current in proteolytically cleaved hENaC.

A, Cells were patched in the whole cell mode; inward current was elicited at -100 mV. AP301 (up to 200 nM) did not induce inward sodium current from hENaC endogenously expressed in (HNEC) RPMI-2650 cells. B, quantitation of 200 nM AP301-induced and 10  $\mu$ M amiloride-sensitive currents in quiescent hENaC endogenously expressed in RPMI-2650 cells (n=18). C, application of 120 nM AP301 following treatment with 100  $\mu$ g/ml trypsin, and amiloride (10  $\mu$ M) block of AP301-induced current. D, quantitation of control (near-silent), 100  $\mu$ g/ml trypsin- and 200 nM AP301-induced currents and 10  $\mu$ M amiloride-sensitive current (in trypsin-cleaved channels following treatment with trypsin, hENaC endogenously expressed in RPMI-2650 cells) (n=11). \*\*\*,  $p < 0.001$  compared with control as determined by t test.

### Figure 5

#### Amiloride-sensitive AP301-induced current activation in transiently and endogenously expressed ENaC.

A, AP301 activated the Na<sup>+</sup> current in transiently expressed  $\alpha\beta\gamma$ -hENaC in HEK-293 and CHO cells with similar efficacy and potency ( $EC_{50}$  in HEK:  $54.7 \pm 2.2$  nM, n=7, and in CHO:  $58.1 \pm 1.9$  nM, n=9) as endogenously expressed in A549 cells ( $EC_{50}$   $54.7 \pm 1.0$  nM, n=11). The respective control currents were  $78.2 \pm 5.9$  pA in HEK-293,  $109.7 \pm 11.0$  pA in CHO, and  $118.5 \pm 8.3$  pA in A549 cells. Cells were patched in the whole cell mode; inward current was elicited at -100 mV. B, dose-response curves of amiloride-inhibited current through  $\alpha\beta\gamma$ -

MOL # 89409

hENaC (n=9) expressed in HEK-293 cells before (control, squares) and after the activation with AP301 (120 nM, circles).

## Figure 6

### **AP301 activation of ENaC requires pore-forming $\alpha$ - or $\delta$ -subunits co-expression.**

A, Amiloride (10  $\mu$ M)-sensitive current in different subunits and subunit combinations expressed in HEK-293 cells. Cells were patched in the whole cell mode; inward current was elicited at -100 mV. B, AP301 (120 nM)-induced current.  $\alpha$ -,  $\beta$ -  $\gamma$ - and  $\delta$ -subunits of hENaC were expressed in HEK cells alone and in all possible combinations. Highest amount of amiloride-sensitive current was only detectable in triplet subunit expressions. Dual combinations only showed an increase in current in presence of the pore-forming  $\alpha$ - or  $\delta$ -subunits. By contrast  $\beta$  and  $\gamma$  alone or expressed together showed a very low level of amiloride-sensitive current (n= 19 to 21). \*\*\*,  $p < 0.001$  compared with  $\alpha\beta\gamma$ -hENaC

## Figure 7

### **The post translationally modified extracellular loop is critical for AP301 activation of hENaC.**

A, In-side out and out-side out patch clamp configurations; inward current was elicited at -100 mV. The effect of AP301 (120 nM) was studied in inside-out and outside-out patches in A549 cells. Mean values of total current are shown. Control current in outside-out patches was  $5.1 \pm 1.3$  pA (n= 17) and in inside-out patches  $4.9 \pm 2.3$  pA (n=17). Application of AP301 (120 nM) in the bath solution showed activated hENaC current ( $15.3 \pm 0.9$  pA, n= 17,  $p < 0.001$ ) in outside-out patches. In contrast, inside-out patch clamp configuration did not yield increased total inward current ( $4.8 \pm 5.7$  pA, n=13). B, quantitation of 120 nM AP301-induced amiloride (10  $\mu$ M)-sensitive currents without and following treatment with 100 units PNGase F for 1 to 5 minutes in endogenously expressed hENaC in A549 cells (n=17,  $p < 0.001$ , AP301 treated cells compared with and without PNGase F treatment). C, quantitation of 120 nM AP301-induced amiloride(10  $\mu$ M)-sensitive currents without and

MOL # 89409

following treatment with 100 units PNGase F in transiently expressed hENaC in HEK-293 cells ( $n=19-21$ ,  $p<0.001$ , AP301 treated cells compared with PNGase F and AP301 treated cells). D, quantitation of 120 nM AP301-induced amiloride (10  $\mu$ M)-sensitive currents without and following treatment with 100 units PNGase F for 1 to 5 minutes and in non-transfected HEK-293 cells ( $n=31$ ). \*\*\* $p<0.001$

MOL # 89409

**Table 1:** Effect of TNF- $\alpha$ , AP301 and AP318 on single channel kinetics at  $E_h = -60$  mV (n=3-5).

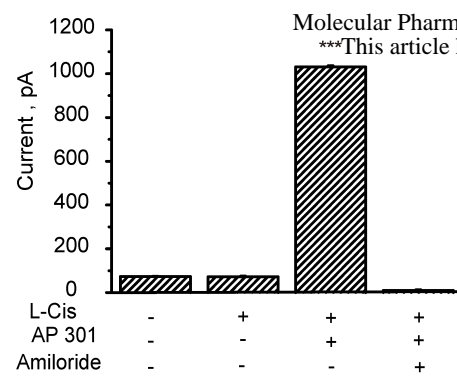
	Control	TNF- $\alpha$	AP301	AP318
$P_o$	$0.37 \pm 0.03$	$0.77 \pm 0.08^{***}$	$0.69 \pm 0.05^{***}$	$0.78 \pm 0.05^{***}$
Mean open time (ms)	$2.2 \pm 0.9$	$23.5 \pm 4.5^{***}$	$24.3 \pm 4.8^{***}$	$26.5 \pm 4.3^{***}$
Number of bursts	$993 \pm 105$	$1274 \pm 259^*$	$2365 \pm 419^{***}$	$1966 \pm 402^{**}$
Events in burst	$7.2 \pm 1.7$	$46.3 \pm 4.3^{***}$	$32.3 \pm 5.0^{***}$	$16.1 \pm 4.9^{**}$
Duration of burst (ms)	$5.7 \pm 1.3$	$210.6 \pm 47.8^{***}$	$47.9 \pm 1.4^{***}$	$42.2 \pm 12.5^{***}$
Mean intra-burst interval (ms)	$0.29 \pm 0.03$	$0.60 \pm 0.1^{**}$	$0.63 \pm 0.03^{***}$	$0.60 \pm 0.12^{**}$

\*  $p < 0.05$ , \*\*  $p < 0.01$ , \*\*\*  $p < 0.001$

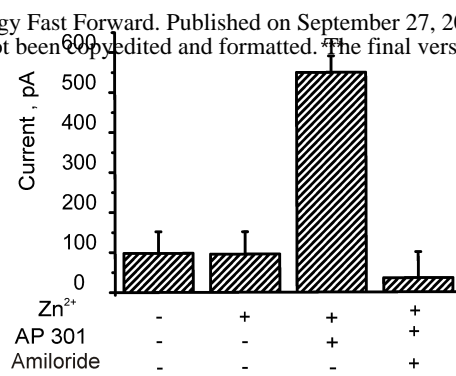


Figure 1

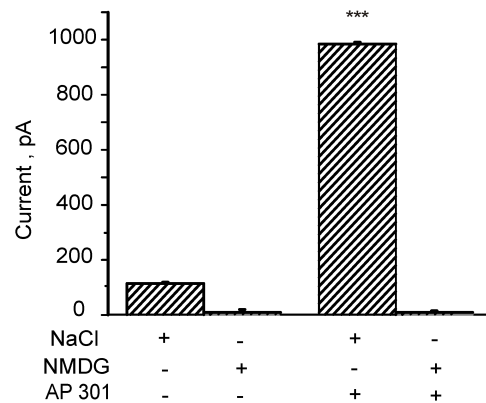
A



B



C



D

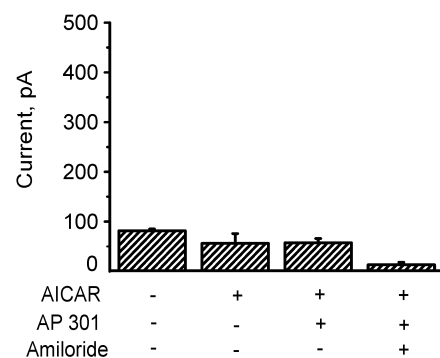
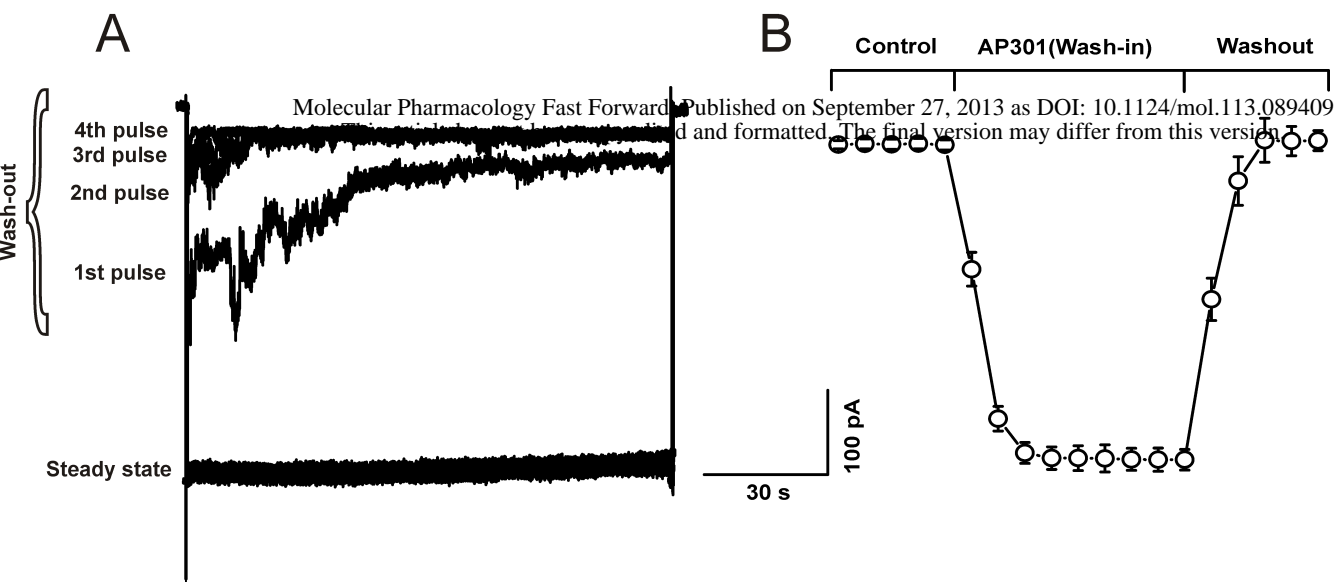


Figure 2



**Figure 3**

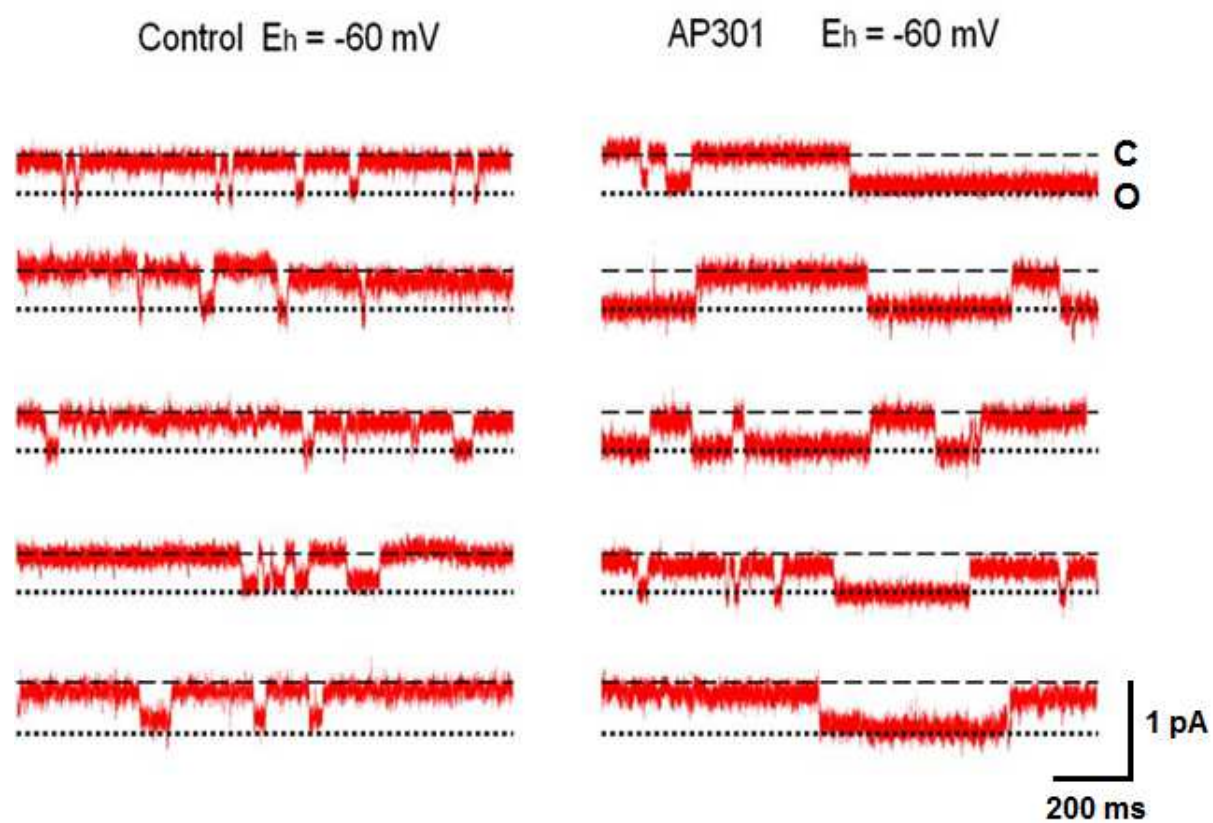
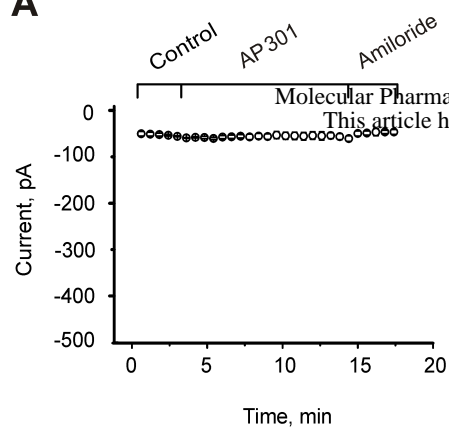
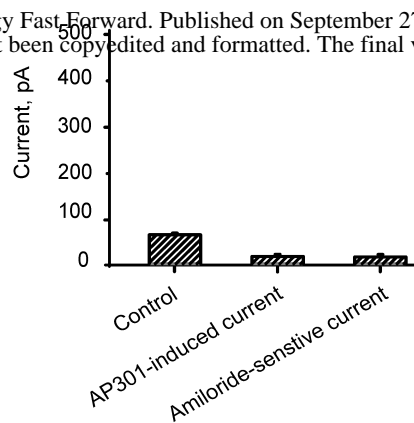


Figure 4

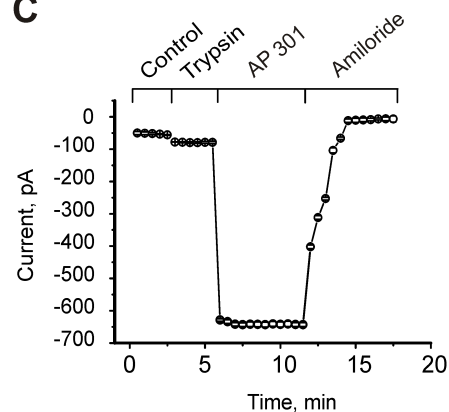
A



B



C



D

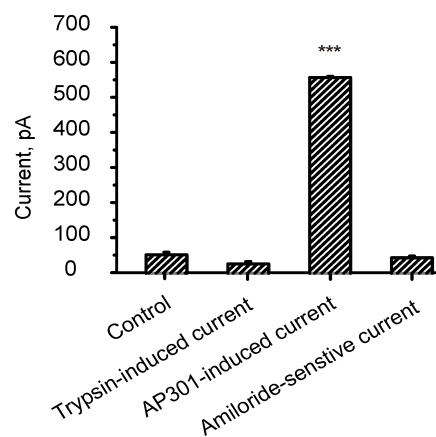
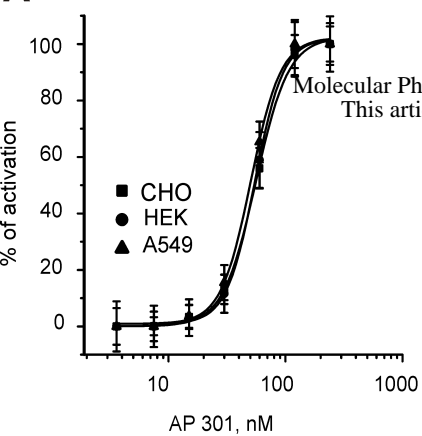
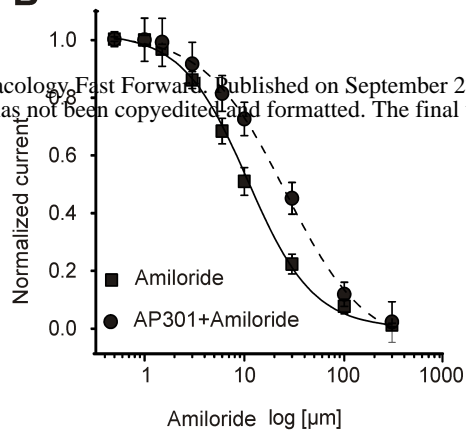


Figure 5

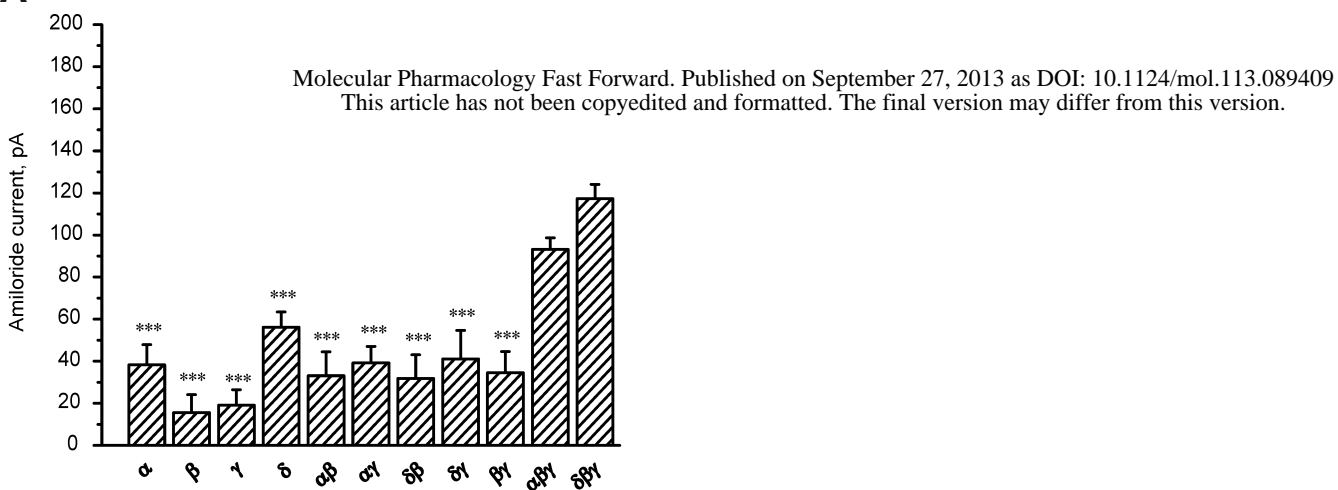
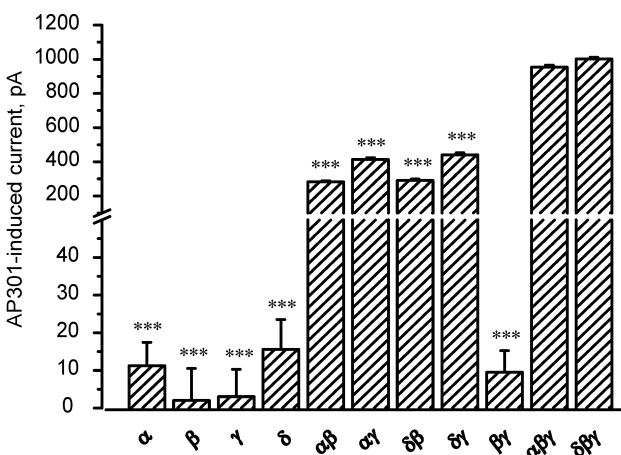
**A**



**B**



Molecular Pharmacology Fast Forward. Published on September 27, 2013 as DOI: 10.1124/mol.113.089409  
This article has not been copyedited and formatted. The final version may differ from this version.

**Figure 6****A****B**

**Figure 7**